*Communication*

# A Semi – Three Dimensional (3D) Bioprinted Neurocardiac System for Tissue Engineering of a Cardiac Autonomic Nervous System (CANS) Model

**Ivana Hernandez [1,2], Salma P. Ramirez [1,2], Wendy V. Salazar [1], Sarahi Mendivil [1], Andrea Guevara [1], Akshay Patel [1,3], Carla D. Loyola [1,2], Zayra N. Dorado [1,2] and Binata Joddar [1,2,4]***

[1] Inspired Materials and Stem-Cell Based Tissue Engineering Laboratory (IMSTEL), The University of Texas at El Paso, El Paso, TX, 79968, USA; ihernadez56@miners.utep.edu, spramirez6@miners.utep.edu, wvsalazar@miners.utep.edu, smendivil2@miners.utep.edu, aguevara10@miners.utep.edu, apatel953@ucsb.edu, ccloyola@utep.edu, zndorado@miners.utep.edu, bjoddar@utep.edu

[2] Department of Metallurgical, Materials, and Biomedical Engineering, M201 Engineering, The University of Texas at El Paso, 500 W. University Avenue, El Paso, TX, 79968, USA; ihernadez56@miners.utep.edu, spramirez6@miners.utep.edu, ccloyola@utep.edu, zndorado@miners.utep.edu, bjoddar@utep.edu

[3] Department of Chemical Engineering, University of California, Santa Barbara, CA, 93106, USA; apatel953@ucsb.edu

[4] Border Biomedical Research Center, The University of Texas at El Paso, 500 W. University Avenue, El Paso, TX, 79968, USA; bjoddar@utep.edu

* Correspondence: bjoddar@utep.edu

**Abstract:** In this study, we designed a functional neuro-cardiac model to help us examine the role of neuronal regulation and confirm the importance of neural innervation techniques for cardiac tissue regeneration. A three-dimensional (3D) bioprinted neuro-cardiac scaffold composed of a mixture of gelatin-alginate and alginate-genipin-fibrin hydrogels was developed with a 2:1 ratio of AC16 cardiomyocytes (CMs) and retinoic acid differentiated SH-SY5Y neuronal cells (NCs) respectively. A unique semi-3D bioprinting approach was adopted where the CMs were mixed in the cardiac bioink and printed using an anisotropic accordion design to mimic the physiological tissue architecture in vivo. The voids in this 3D structure were methodically filled in using a NCs-gel mixture and cross-linked. Confocal fluorescent imaging using Microtubule-associated protein 2 (MAP-2) antibodies for labeling NCs, and the MyoD1 antibody for CMs revealed functional coupling between the two cell types in the final cross-linked structure. This data confirmed the development of a physiologically functional neuro-cardiac model that can be used to study neuro-cardiac modulation under physiological and pathological conditions.

**Keywords:** 3D bioprinting; neuro-cardiac junctions; 3D tissue model; cardiomyocytes; neuroblastoma cells

## 1. Introduction

The Cardiac Autonomic Nervous System (CANS) controls hemodynamic changes via the regulation of heart rate among other important functions. This is mostly because sympathetic and parasympathetic impulses between the heart and the peripheral and central nervous systems are carefully balanced, regulating the autonomic control of the heart through multiple levels of feedback loops [1,2]. More specifically, the sympathetic ganglia combine central and peripheral inputs to send signals to the heart through motor neurons that target cardiomyocytes. The manner in which neural information is transmitted to the corresponding cardiac targets is determined by this communication. The relationship between these types of cells, cardiomyocytes and neurons have not yet been comprehensively studied [3] in the context of ischemic heart disease or chronic coronary syndrome, which are a few of the most prevalent causes of heart failure. This condition lowers blood oxygen levels and weakens the myocardial tissue and contractile forces generated [4]. There are currently two common approaches that are adopted to counteract the effects of this disease, such as the use of

 doi:10.20944/preprints202306.0887.v1



antianginal drugs. The other technique entails surgical interventions such coronary angiography, followed by either percutaneous coronary intervention or coronary artery bypass grafting [5]. Although not prevalent, cardiac tissue engineering with neuronal innervation also seems to be a potential therapeutic strategy towards the treatment of ischemic heart disease. Thus, in this study, our goal was to co-culture cardiomyocytes and neuronal cells in a 3D model that can be successfully extrapolated towards the biofabrication of a CANS model using bioprinting. It is hypothesized that such an in-vitro tissue-engineered CANS model can eventually strengthen our understanding and pave the way for the development of a regenerative medicine-based strategy for the treatment of ischemic heart disease in clinical settings. In this presented work, an original approach using a semi-three-dimensional (3D) bioprinting strategy was adopted to fabricate a neuro-cardiac scaffold made of two different bioinks. The cardiac bioink was composed of Gelatin-Alginate and contained AC16 cardiomyocytes (CMs), and the neuronal bioink was composed of Alginate-Genipin-Fibrin and retinoic acid differentiated SH-SY5Y neuronal cells (NCs). The neuro-cardiac scaffold was developed using a 2:1 mixture ratio of both cell types (Cardiomyocytes: Neurons) to improve heterocellular interactions between both cell lines. By incorporating multiple arrowheads into the design, the scaffold design was intended to replicate the geometry and morphology of myocardial tissue [6]. It is expected that this arrowhead design will promote effective networking between neurons and cardiomyocytes in comparison to a 2D platform [7]. Cell growth, function, maintenance, and heterocellular coupling would have steadily risen in all regions of the structure as a result of the circulation of the mixed growth media from the interior to the exterior of the scaffold design [8] allowing effective communication between the two cell types leading to the formation of a CANS tissue-engineered model.

## 2. Materials and Methods

### *2.1. Materials*

For making the cardiac bioink the following materials and supplies were used including Medium Viscosity Alginate (MVG) (Sigma Aldrich, St. Louis, MO), gelatin (Sigma-Aldrich, St. Louis, MO), and 3 mL syringe-printing cartridges with a 20G tapered conical nozzle (CELLINK, Blacksburg, VA). For the cardiac bioink crosslinking solution, 1X PBS (Fisher Bioreagents), and calcium chloride dihydrate (Fisher Chemical, Germany) were used. To create the ionic crosslinking solution, calcium chloride (CaCl2) was added into 1X PBS having a final concentration of 100 mM.

For making the neuronal bioink, Low Viscosity Alginate (LVG) was used with 1X tris-buffered saline (component 1), 25 mg/mL genipin (component 2), and 50 mg/mL fibrinogen (component 3). Crosslinker components also included 25 mg/mL chitosan with approximately 560 mg/mL β-Glycerophosphate (component A), and 1000 U/mL thrombin with 20 mg/mL calcium chloride (component B). Components 1-3 and A-B were provided by Axolotl Sciences (Victoria, BC) and were developed previously by the Willerth Lab at the University of Victoria *[9,10]*. The following equipment and reagents were used for all cellular experiments: Plastic petri dishes (ThermoFisher Scientific, Waltham, MA) and 1X PBS (Cytiva HyClone™, Logan, Utah); serological pipettes of sizes 1ml, 5ml, and 10ml; 6 well plates; (ThermoFisher Scientific, Waltham, MA). The crosslinker's purpose for both bioinks was to sequester the structure together such that the shape would hold when exposed to non-uniform stress.

Please refer to supplementary section S2.1 for further details on the materials used for making the bioinks, cell culture and passaging, as well as immunostaining.

### *2.2. Preparation of Cardiac Bioink*

The cardiac bioink consisted of medium viscosity alginate (MVG) mixed with gelatin, to make it extrudable under moderate amounts of shear pressure. The bioink contained 10% (w/v) gelatin dissolved in PBS (pH 7.4) with light heat and constant mixing with a magnetic stirrer under sterile conditions. Another solution of 14% (w/v) MVG sodium alginate was made with or without cell suspension in combined growth media in a 5 mL conical tube. Both solutions were combined into a

 doi:10.20944/preprints202306.0887.v1



separate 5 mL conical tube so that the absolute concentration of the bioink was 5% (w/v) gelatin and 7% (w/v) MVG alginate. The mixture was allowed to dissolve overnight at room temperature and then centrifuged at 1200 rpm for 3 min to remove air bubbles. All gels were UV-sterilized for 15 min before loading into printing cartridges or mixing with cells. For cell-based studies, this cardiac bioink was mixed with cells and loaded into a 3 mL syringe-printing cartridge with a 20G tapered conical nozzle. Acellular gels were loaded without mixing cells for material characterization studies. To create the ionic crosslinking solution, calcium chloride (CaCl2) was added into 1X PBS having a final concentration of 100 mM.

*2.3. Preparation of Neuronal Bioink*

The neuronal bioink was prepared according to previously published works [9,10]. All reagents were previously prepared, sterilized and provided by Axolotl Biosciences (Victoria, BC). Upon receiving, components (see section S2.1) were stored at -20°C. Bioink component 1, and crosslinker components A and B were thawed at 4°C, while bioink components 1 and 2 were thawed at room temperature and at 37°C respectively. For acellular experiments, bioink component 2 in a concentration of 0.3 mg/mL was pipetted into component 1 (0.5% v/v), after mixing these reagents, component 3 (20 mg/mL) was slowly pipetted into the mixture and was once again mixed. For bioprinting, cells were mixed with component 3 and then the cell mixture was added to the mixture of components 1 and 2. For the crosslinker solution, component B (Thrombin: 1.7 U/mL and Calcium Chloride: 19.16 mg/L) was slowly added with a pipette to component A (Chitosan: 19 mg/mL and β-Glycerophosphate: 6.6 mg/mL). Please refer to supplementary S2.1 for details on all components of the neuronal bioink.

*2.4. Semi – Three Dimensional (3D) Bioprinting*

The SolidWorks software was used to design a 3D accordion-like arrowheads scaffold with dimensions of 20 cm (L) x 20 cm (W) and 0.05 cm (H), strut thickness of 0.5 - 1 cm, and spaces of 1 x 2.12 cm, which was bioinspired by the honeycomb-like lattice framework of an in-vivo heart tissue [8,12]. The cardiac bioink was directly extruded into this design onto a 100 x 15 mm petri dish utilizing the BIOX (CELLINK, Blacksburg, VA) 3D bioprinter. The optimal bioprinting settings [13] and parameters can be seen in Table 1.

**Table 1.** Optimized printing parameters.

| Parameter | Specification |
|---|---|
| Nozzle diameter | Tapered 22G |
| Printing speed | 1 mm/s |
| Pressure | 70 kPa |
| Temperature | 32 °C |
| Infill | 25% |

The complexity of the scaffold design was taken into consideration when choosing the printing speed, the nozzle diameter was selected based on the thickness of the design, and the printing pressure and temperature were set based on how easily the bioink was extruded, preventing shear stress, and increasing cell viability [14]. For bioprinting with cells, the cardiac bioink was mechanically mixed with 2 x 10^6 cells / mL in a 5mL conical tube containing 2 mL of bioink and loaded into a sterile 3 mL syringe using a female luer lock connector for printing with parameters found in Table 1. The neuronal bioink was made by mixing 1 x 10^6 cells/mL in 5 mL conical tube containing 3 mL of the bioink. The neuronal bioink laden with cells was deposited on top of the cardiac scaffold using a multichannel pipette and allowed to settle and penetrate the bottom cardiac layer. The bi-layered composite structure was then cross-linked using a crosslinking mixture for both bioinks mixed in a ratio of 2:1 (cardiac: neuronal). For fluorescent imaging, cells were pre-stained with PKH67 Green Fluorescent Cell Linker Mini Kit for differentiated SH-SY5Y cells and PKH26 Red

 doi:10.20944/preprints202306.0887.v1



Fluorescent Cell Linker Mini Kit for AC16 cardiomyocytes by following vendor's recommendations. The 3D bioprinted neuro-cardiac structures were kept immersed in 1 mL combined media (2:1 for cardiac: neuronal) during all culture times.

Following the 3D printing of the cardiomyocyte-specific structure, the neuronal bioink was micropipetted on top of the cardiac scaffold, dispersed evenly throughout the printed surface, and left to sit for a total of two minutes. After fabricating the co-culture layout, the semi-3D printed structure was crosslinked first with the neuronal crosslinker and removed after 1 minute, then the cardiac crosslinker (100 mM CaCl2) was added with a pipette sufficient to cover the whole structure and placed on a belly dancer shaker (IBI SCIENTIFIC, Dubuque, Iowa) at 10 rpm. Once the crosslinker was removed after 5 minutes, the composite crosslinked structure was washed with 1X PBS three times and placed into a 6-well plate for further experimentation.

### *2.5. Material Characterization*

For details on Swelling Analysis (S2.5.1), ATR-FTIR (S2.5.2), and SEM (S2.5.3) please refer to the supplementary section S2.5.

### *2.6. Cell Culture and Passaging*

For details on cell culture and passaging please, refer to supplementary section S2.6.

### *2.7. Fluorescent imaging*

#### 2.7.1. Heterocellular coupling

The total number of heterocellular couplings between the PKH26 (red) stained AC16 cardiomyocytes and the PKH67 (green) stained SHSY-5Y differentiated neuronal cells was assessed in order to analyze the interactions between both cell lines that were placed in the semi–3D bioprinted structures via confocal microscopy imaging. The cells were first fixed by immersing the structures in a 4% paraformaldehyde (PFA) solution for 15 minutes at room temperature, structures were then rinsed thrice with 1X PBS and placed on a Belly Dancer Shaker at 10 rpm for 5 minutes. Samples were counterstained using mounting media with DAPI and placed on glass slides prior to imaging. The average heterocellular cell coupling percentage was calculated by using the following formula:

$$\%\ Coupling = \frac{\#\ of\ CMs\ (red),\ \#\ of\ NCs\ (green)}{total\ \#\ of\ cells\ in\ image} \times 100 \qquad (1)$$

#### 2.7.2. Immunostaining

Immunostaining studies were performed to detect the expression of MyoD1 in AC16 cardiomyocytes and MAP-2 in differentiated SH-SY5Y neurons. The AC16 cardiomyocytes in 3D printed structures were washed with 1X PBS three times and fixed with 4% paraformaldehyde (PFA) solution for 15 minutes at room temperature, structures were rinsed 3 times immersed in 1X PBS and placed on a Belly Dancer Shaker at 10 rpm for 5 minutes. Cells were blocked with blocking solution overnight at 4°C. After removal of the blocking solution structures were rinsed thrice using 1X PBS and placed on a Belly Dancer Shaker for five minutes. The primary antibodies were then added to the samples and incubated overnight at 4°C. The samples were then washed three times with 1X PBS and then incubated for an hour at room temperature with secondary antibodies as outlined earlier in 2.1. The secondary antibody solution was then removed, and the samples were washed again and mounted on glass slides and images were acquired using a confocal fluorescent microscope.

## 3. Results

In this study, our goal was to create a 3D biological in-vitro model representing the "neuro-cardiac junctions" found in the human heart. To achieve these cardiomyocytes and neurons were co-cultured on a bilayered hydrogel structure assembled using a novel semi-3D printing approach consisting of two different bioinks containing cardiomyocytes and neurons and referred to as the

Preprints (www.preprints.org) | NOT PEER-REVIEWED | Posted: 13 June 2023 doi:10.20944/preprints202306.0887.v1



cardiac and the neuronal bioink, respectively. The cardiac bioink was laden with cardiomyocytes mixed in a hydrogel mixture consisting of gelatin and alginate and was crosslinkable by the addition of divalent calcium ions. The neuronal bioink was laden with differentiated SH5YSY neurons mixed alginate, genipin, and fibrin; the hydrogel was crosslinked using chitosan, β-glycerophosphate, thrombin, and calcium chloride. As shown in Figure 1, this work led to the development of a semi-3D printed cardiac-neuronal scaffold for tissue engineering applications. Briefly, the cardiac scaffold was 3D printed and deposited using the cardiac bioink and based on the stl design depicted in Figure 1. Next, the neuronal bioink was pipetted and layered on top of the cardiac scaffold and allowed to confirm to the shape of this basal layer and fill in all gaps. This step took a total of 1-2 mins. Finally, the 3D composite bilayered structure was crosslinked using a mixture of crosslinking agents for the cardiac and the neuronal bioinks mixed in a ratio of 1:1. The crosslinking step incurred an additional two minutes, and the endpoint of this step was determined by visual confirmation of the scaffold turning blue (confirmed by genipin crosslinking [17]) indicating the formation of the composite crosslinked cardiac-neuronal scaffold. The crosslinker's purpose was to sequester the structure together such that the shape would hold when exposed to non-uniform stress.

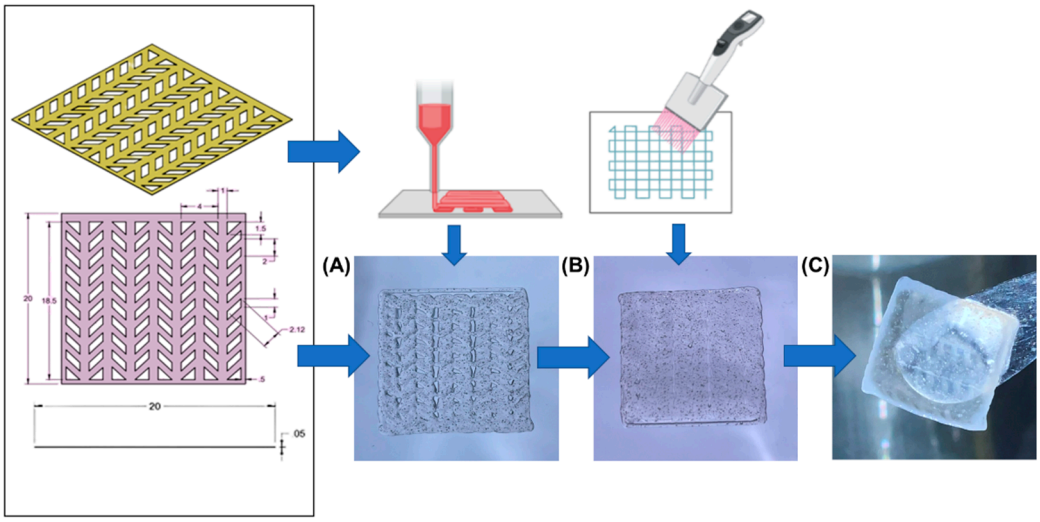


**Figure 1.** Semi 3D printed neuro-cardiac structure. Cardiac bioink is 3D bioprinted (based on the STL design shown) and placed on bottom (A) while neuronal bioink is pipetted and layered on top (B). Composite 3D structure after crosslinking can be observed in (C).

Fourier Transform Infrared (FTIR) spectroscopy not only confirmed each of the hydrogel's chemistry and crosslinking (Figure 2 A, B), but it also identified the chemical compatibility between the two hydrogels. The most eminent peaks that were identified included a broad and stretched peak at ~3300 cm-1 that confirmed the C-H and O-H stretch [18]. Another peak was evident at ~1020 cm-1 and corresponded towards the C-O-C stretching [19] whereas the relatively small peak at ~1315 cm-1 implied the presence of C-O stretching that is typical to alginate chemistry [20]. The peak at ~1620 cm-1 corresponded to the C=N Schiff's Base and is typical to gelatin [21], detected most accurately in the cardiomyocyte crosslinked structure. The peak at ~1500 cm-1 points towards the presence of aromatic ring related bonds and was found in the neuronal bioink possibly due to genipin [22]. All these peaks confirmed successful crosslinking and were distinct when compared between crosslinked and non-crosslinked structures.

Preprints (www.preprints.org) | NOT PEER-REVIEWED | Posted: 13 June 2023 doi:10.20944/preprints202306.0887.v1



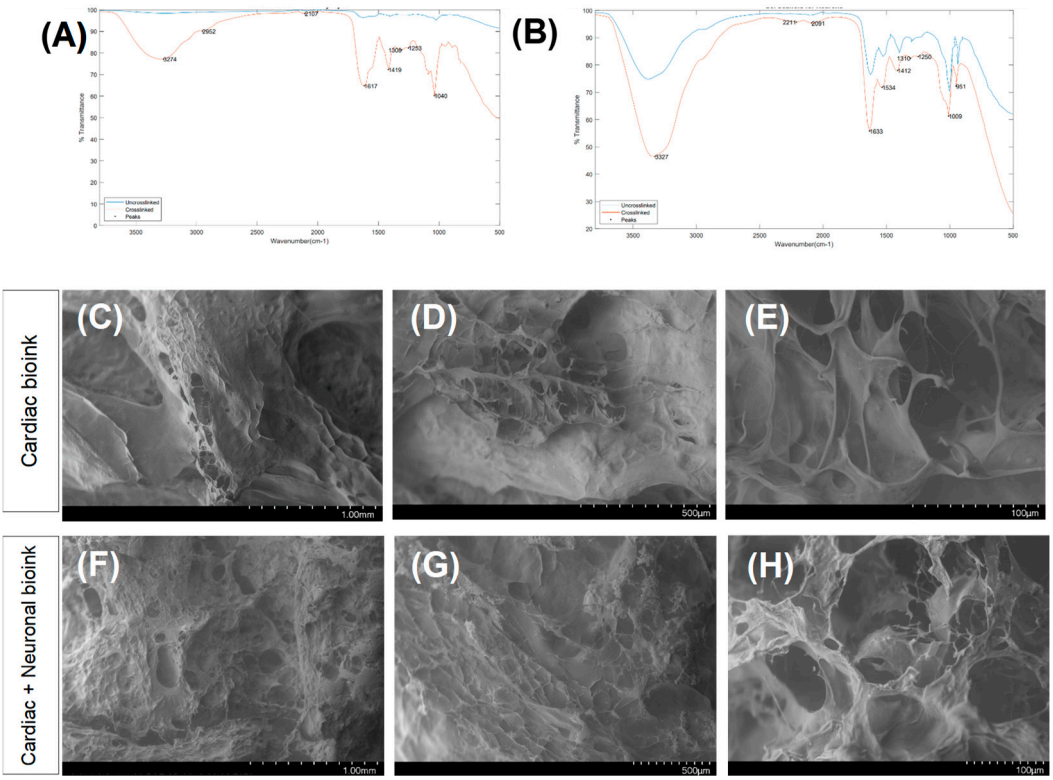


**Figure 2.** FTIR analysis results for scaffolds printed using the bioink for cardiac cells (A), and the bioink for the neurons (B). A comparison between non-crosslinked and crosslinked scaffolds are depicted blue and red respectively. SEM images of cardiac bioprinted structure (C-E) and neurocardiac scaffold (F-H).

As shown in the SEM images in Figure 2 C-E, the cardiac scaffolds revealed design specificity with the stl. file that was used to guide the accordion design of this scaffold. The pores and struts present in the cardiac scaffold were greater compared to the composite neuro-cardiac scaffold depicted in Figure 2 F-H. In the composite neuro-cardiac scaffold the voids present in the cardiac counterpart appeared to be filled in as confirmed by the smaller pores distributed throughout the imaged sample surface.

Figure 3 depicts results obtained from morphological and mechanical characterization studies done on the composite and crosslinked neuro-cardiac scaffolds using swelling and rheological analyses respectively. Figure 3(A) shows swollen scaffolds at varying time points that are graphically represented in 3(B) below. Both figures and graphs confirm the retention of the structural fidelity of the scaffolds during the entire study period, however, the maximum swelling occurred after 4-days, and the trends seemed to suggest a sustained degradation of the structure when studied after 7-days. Shown in 3(C) are the storage and loss moduli and in 3(D) the complex viscosity for 3D bioprinted and cross-linked neuro-cardiac scaffold at varying time points are depicted. The storage modulus is a measure of how much energy a sample needs to undergo distortion while the loss modulus accounts for the energy lost between the loading and unloading cyclic strain. Complex viscosity indicates the overall resistance to flow or deformation of the material, with higher values representing more viscous or less flowable materials. It is also frequency-dependent and was determined by subjecting the scaffolds to oscillatory shear stress. As shown by our results in 3(C) and (D) the reduction in storage and loss moduli as well as the complex viscosity when assayed after 7-days confirmed the sustained biodegradation of the composite crosslinked scaffolds. However, the storage modulus was significantly higher in value compared with the loss modulus at all-time points studied confirming the presence of a viscoelastic structure that had more solid content compared with its liquid content.

Preprints (www.preprints.org) | NOT PEER-REVIEWED | Posted: 13 June 2023 doi:10.20944/preprints202306.0887.v1



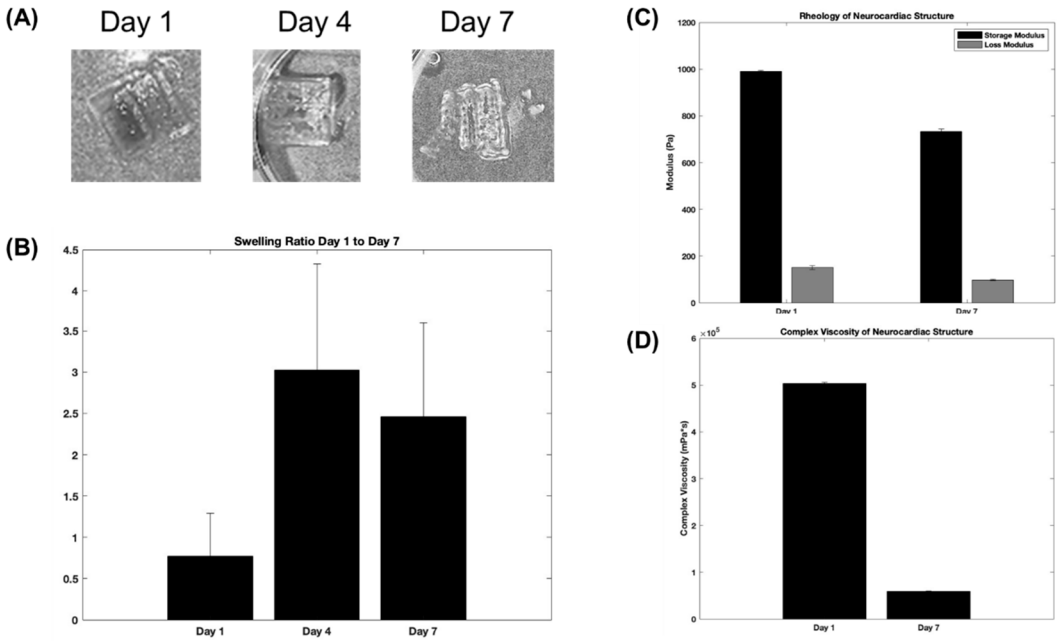


**Figure 3.** Swelling and Rheological Analyses. Shown are representative structures at varying time points (A), that are included in the graph below (B). Shown in (C) are the Storage and Loss Moduli plotted and in (D) the Complex Viscosity for 3D bioprinted and cross-linked neuronal-cardiac scaffold at varying time points.

Figure 4 (A, B) shows characteristic images captured from 3D neuro-cardiac cultures with neuronal cells stained green (PKH67), cardiomyocytes in red (PKH26) and nuclei in blue (DAPI). Regions with an overlap of both colors (red circles) confirmed the neuro-cardiac heterocellular coupling between both cell types studied. Shown in 4 (C, D) are representative images from the 2D cultures of neuronal and cardiac cells respectively. These results confirmed the neuro-cardio coupling relationship in the 3D crosslinked scaffolds in comparison with 2D cultures. Cardiomyocytes were found to be at the bottom and neurons were detected at the top of the 3D structures as confirmed by confocal microscopic imaging. Moreover, the cells retained their viability in the accordion-designed scaffold which may have also helped retain culture viability. Shown in (E) is the quantification of heterocellular coupling shown in Figure 4 (A) and (B). The extent of the heterocellular coupling between neuronal and cardiac cell cultures was quantified and depicted in 4(E). Our results depict similar trends as reported by earlier published studies by others and the extent of heterocellular coupling was enhanced in the 3D scaffolds in comparison to the 2D cultures (~5%, data not included).

Characteristic cardiac and neuronal cell phenotype and morphology that were involved in the heterocellular cell coupling were confirmed with confocal microscopic imaging via immunostaining. Results from 3D neuro-cardiac cultures are shown in Figure 5(A-D) showing AC16 cardiomyocytes (red) as shown in (C), and SHSY5Y neurons (green) shown in (B). All cell nuclei were stained using DAPI (blue) as depicted in (A) and the merged result showing both cell types is depicted in (D) and (E). Cardiomyocytes were probed using their expression of the MyoD1 protein, while the neurons were identified based on their expression of the MAP2 protein. Shown in Supplementary Figure 1 are the immunostaining results from 2D cultures showing SHSY5Y neurons (A) with neurite projections identified with MAP2, and (B) showing clustering of neurons confirming their differentiation. Shown in (C) are cardiomyocytes cultured in 2D controls and identified with their MyoD1 expression.

Preprints (www.preprints.org) | NOT PEER-REVIEWED | Posted: 13 June 2023 doi:10.20944/preprints202306.0887.v1



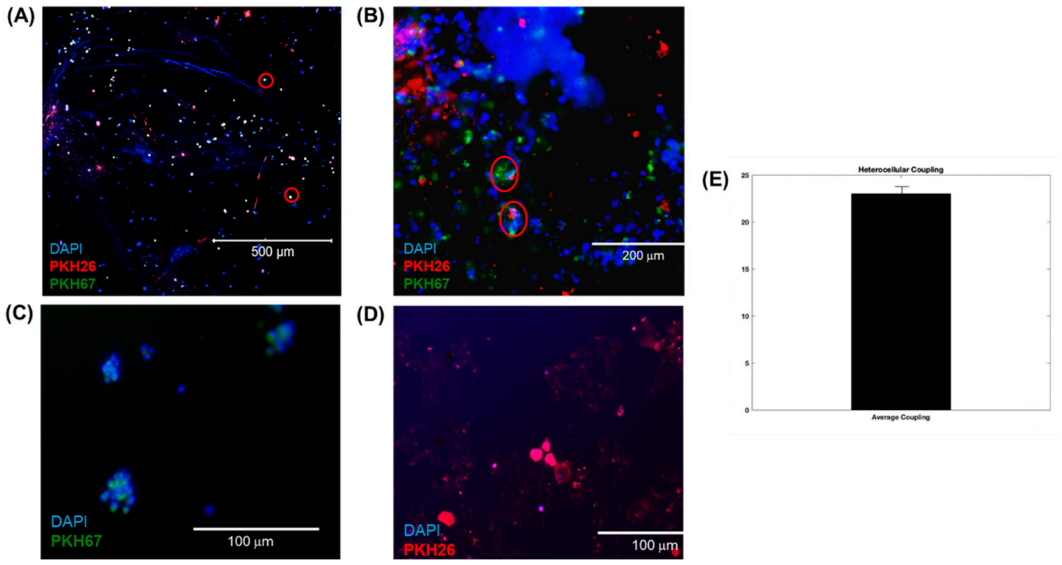


**Figure 4.** (A) 3D Neuro-Cardiac cultures showing an image of neuronal cells stained green (PKH67), cardiomyocytes stained in red (PKH26) and nuclei in blue (DAPI). Regions with a yellowish color (red circles) show the neuro-cardiac heterocellular coupling between both cell types studied. Shown in (B) is a representative image from a 2D Neuro-Cardiac culture. Cardiac cells are located at the bottom and neuron cells are located at the top. Shown in (C) and (D) are indicative images from the 2D cultures of neuronal and cardiac cells respectively. Shown in (E) is the quantification of heterocellular coupling shown in (A).

## 4. Discussion

3D bioprinting offers several advantages over conventional tissue engineering via its potential in printing complex multicellular structures and even hollow organs. However, there are still some limitations such as non-uniform seeding of cells into constructs, placement of different types of cells in defined position, and not being able to reconstruct complex 3D organs.

In this work, both cardiac and neuronal cell types were strategically incorporated within their respective bioinks for a semi-3D bioprinting technique. Since extrusion-based 3D bioprinting has been demonstrated to have no negative effects on cell survival, it has been widely used with cardiac cells [8]. Additionally, the alginate – gelatin mixture facilitates the printing process yielding a great support for cardiac cell survival by reducing shear stresses [23]. On the other hand, the specialized bioink for neuronal cells is comparable with the extra cellular matrix present in cerebral tissue [24]. Nonetheless, given its low viscosity and difficult to extrude core components, microfluidic bioprinters are the most suitable option for the fabrication of neural constructs [24]. The essential benefit of this semi-3D bioprinting approach is that it eliminates the need for two different bioprinting approaches and specialized equipment to biofabricate a single structure with two types of biomaterials with differing viscosities.

Despite its low viscosity and poor mechanical handling properties of the neuronal bioink, once incorporated and crosslinked in the neuro-cardiac scaffold the construct offered ease of handling and tissue culture, making it easier to manipulate during in vitro studies. Swelling and degradation analysis showed structural integrity throughout the duration of seven days for the composite neuro-cardiac scaffold.

In order to achieve complex geometries through 3D bioprinting, it is essential for the bioink to maintain its structure and stability after printing and crosslinking. To confirm this behavior, we investigated and compared the increase in storage moduli for both cardiac and neuronal bioinks after crosslinking, as reported in a previously published study [25]. However, the extrusion-based cardiac bioink demonstrated a higher storage modulus, indicating more elastic-like behavior (G') [25] when compared to the neuronal bioink [25]. The observed increase in storage modulus in the cardiac bioink can be attributed to a sustained swelling and degradation pattern of the composite neuro-cardiac scaffold in comparison to the neuronal bioink alone.

 doi:10.20944/preprints202306.0887.v1



FTIR spectroscopy gathers graphical data by sending a range of wavelengths from which specific bonds within the material absorb [18–22]. For instance, a wave with wavenumber, which is the reciprocal of the wavelength, of 1050 cm-1 will be absorbed by the primary alcohol functional group (-OH). This is reflected in the % transmittance, as the sensor at the other end of the FTIR machine records only a fraction of the initial wave sent out. The crosslinking of the hydrogels corresponding to the larger peaks was confirmed via FTIR analysis. This meant that the cross-linked bonds absorbed a greater fraction of the waves sent out compared to the uncrosslinked structures. It is conjectured that crosslinking lowers the free energy of the functional groups, making the bonds vibrate more visibly for the FTIR spectroscopy to record. Moreover, the functional groups verified by FTIR spectroscopy support that relatively strong intermolecular forces, such as hydrogen bonding and electrostatic attractions, arise when the two bioinks are layered upon each other.

The interaction of cells between differentiated neurons and cardiomyocytes are emphasized by the immunostaining results. A successful heterocoupling phenomenon was demonstrated between these essential cell types as it is found normally in physiological cardiac tissue innervated by the branches of the autonomic nervous system [26]. In previous studies, the heterocellular interactions between human induced pluripotent stem cell (hiPSC) derived sympathetic neurons and hiPSC cardiomyocytes has been demonstrated in a 2D co-culture set-up [7]. This prior study in comparison with our results, suggest that the adoption of a semi 3D bioprinted strategy enhanced the heterocellular coupling significantly by allowing their systematic positioning, where cardiomyocytes were placed at the bottom and neurons at the top.

Reportedly, this unique 3D bioprinting approach has not been implemented before with cardiac and neuronal cells. Owing to the lack of availability of such models, very few physiological platforms exist for understanding the mechanisms underlying sympathetic interactions of neurons with cardiovascular units [7]. The semi-3D bioprinting approach presented in this study offers an immense potential to co-culture cardiomyocytes and neurons by combining several cell-biomaterials into a single engineered structure. This will pave the way for the study of how neuronal regulations or dysregulations can contribute to various cardiovascular diseases and will enable further research into how the autonomic nervous system controls heart function. This study provides a tissue on a chip platform y to discover and create novel treatment approaches using 3D neuro-cardiac models.

## 5. Conclusions

To better understand the connections between the heart and brain tissues, a semi-3D bioprinted neurocardiac tissue model was created in this study employing cardiomyocytes combined in an alginate-gelatin hydrogel and neurons mixed in an alginate-genipin-fibrin hydrogel. The 3D scaffolds-maintained cell survival, function, and phenotypes while displaying structural and mechanical integrity. Additionally, the structure successfully demonstrated heterocellular interaction between neurons and cardiomyocytes. In a variety of applications including drug screening and tissue engineering, this semi-3D bioprinted tissue has the potential to be a useful model for examining cell behavior and function.

**Supplementary Materials:** The following supporting information can be downloaded at: www.mdpi.com/xxx/s1, Figure S1: Immunostaining results confirmed via confocal microscopic imaging from 3D Neuro-Cardiac cultures (A-D) showing AC16 cardiomyocytes (MYO D1+Alexa Fluor 647: Red) as shown in (C), and SHSY5Y neurons (MAP-2+Alexa Fluor 488: Green) as shown in (B). All cell nuclei are stained using DAPI (blue) as depicted in (A) and a merged result of both cell types is depicted in (D) and (E); Figure S2: Immunostaining results from 2D cultures showing SHSY5Y neurons (A) with neurite projections, and (B) showing clustering of neurons confirming their differentiation. Shown in (C) are cardiomyocytes cultured in 2D controls.

**Author Contributions:** Conceptualization, methodology, software, formal analysis, investigation I.H, S.P.R., W.V.S., S.M., A.P., Z.N.D., C.DL., and B.J.; resources, B.J.; writing—original draft preparation, I.H., and B.J.; writing—review and editing, I.H., and B.J.; visualization, I.H., and B.J.; supervision, B.J.; project administration, B.J.; funding acquisition, B.J. All authors have read and agreed to the published version of the manuscript.

**Funding:** This research was funded by the National Science Foundation (NSF), award number 1854008.

**Data Availability Statement:** All data analyzed or generated during the study are presented in the manuscript and in the online supplementary section.

**Acknowledgments:** The neuronal bioink, related protocols, and guidance for working with it were graciously provided by Axolotl Biosciences, UVIC, Victoria, Canada.

**Conflicts of Interest:** The authors declare no conflict of interest.

## References

1. Qin, M., C. Zeng, and X. Liu, The cardiac autonomic nervous system: A target for modulation of atrial fibrillation. Clinical Cardiology, 2019. 42(6): p. 644-652.
2. Aksu, T., et al., Intrinsic cardiac autonomic nervous system: what do clinical electrophysiologists need to know about the "heart brain"? Journal of cardiovascular electrophysiology, 2021. 32(6): p. 1737-1747.
3. Zaglia, T. and M. Mongillo, Cardiac sympathetic innervation, from a different point of (re) view. The Journal of physiology, 2017. 595(12): p. 3919-3930.
4. Chaudhry, M., Heart failure. Curr Hypertens Rev 15 (1): 7. 2019.
5. Antman, E.M. and E. Braunwald, Managing stable ischemic heart disease. N Engl J Med, 2020. 382(15): p. 1468-1470.
6. AnilKumar, S., et al., The applicability of furfuryl-gelatin as a novel bioink for tissue engineering applications. Journal of Biomedical Materials Research Part B: Applied Biomaterials, 2018.
7. Winbo, A., et al., Functional coculture of sympathetic neurons and cardiomyocytes derived from human-induced pluripotent stem cells. American Journal of Physiology-Heart and Circulatory Physiology, 2020. 319(5): p. H927-H937.
8. Alonzo, M., et al., 3D Biofabrication of a Cardiac Tissue Construct for Sustained Longevity and Function. ACS Applied Materials & Interfaces, 2022. 14(19): p. 21800-21813.
9. Chrenek, J., et al., Protocol for printing 3D neural tissues using the BIO X equipped with a pneumatic printhead. STAR Protocols, 2022. 3(2): p. 101348.
10. Abelseth, E., et al., 3D printing of neural tissues derived from human induced pluripotent stem cells using a fibrin-based bioink. ACS Biomaterials Science & Engineering, 2018. 5(1): p. 234-243.
11. Qin, C., et al., A Cell Co-Culture Taste Sensor Using Different Proportions of Caco-2 and SH-SY5Y Cells for Bitterness Detection. Chemosensors, 2022. 10(5): p. 173.
12. Anil Kumar, S., et al., A comparative study of a 3D bioprinted gelatin-based lattice and rectangular-sheet structures. Gels, 2018. 4(3): p. 73.
13. Fakhruddin, K., M.S.A. Hamzah, and S.I. Abd Razak. Effects of extrusion pressure and printing speed of 3D bioprinted construct on the fibroblast cells viability. in IOP Conference Series: Materials Science and Engineering. 2018. IOP Publishing.
14. Zhang, B., et al., Micro-and nanotechnology in cardiovascular tissue engineering. Nanotechnology, 2011. 22(49): p. 494003.
15. Xicoy, H., B. Wieringa, and G.J. Martens, The SH-SY5Y cell line in Parkinson's disease research: a systematic review. Molecular neurodegeneration, 2017. 12: p. 1-11.
16. Agholme, L., et al., An in vitro model for neuroscience: differentiation of SH-SY5Y cells into cells with morphological and biochemical characteristics of mature neurons. Journal of Alzheimer's disease, 2010. 20(4): p. 1069-1082.
17. Muzzarelli, R.A.A., et al., Genipin-Crosslinked Chitosan Gels and Scaffolds for Tissue Engineering and Regeneration of Cartilage and Bone. Marine drugs, 2015. 13(12): p. 7314-7338.
18. Ahmed, M. Khalique, et al. "Fourier transform infrared and near-infrared spectroscopic methods for the detection of toxic diethylene glycol (DEG) contaminant in glycerin based cough syrup." Spectroscopy 24.6 (2010): 601-608.
19. Liang, C. Y., and R. H. Marchessault. "Infrared spectra of crystalline polysaccharides. II. Native celluloses in the region from 640 to 1700 cm.− 1." Journal of polymer science 39.135 (1959): 269-278.
20. Yudiati, E., et al. "Accelerating The Physilogical Properties of Sodium Alginate Paste by Thermal Method and Microwave Irradiation." IOP Conference Series: Earth and Environmental Science. Vol. 246. No. 1. IOP Publishing, 2019.
21. Walter, Timothy J., and Mark S. Braiman. "Anion-protein interactions during halorhodopsin pumping: halide binding at the protonated Schiff base." Biochemistry 33.7 (1994): 1724-1733.
22. Mi, Fwu-Long, Shin-Shing Shyu, and Chih-Kang Peng. "Characterization of ring-opening polymerization of genipin and pH-dependent cross-linking reactions between chitosan and genipin." Journal of Polymer Science Part A: Polymer Chemistry 43.10 (2005): 1985-2000.
23. Anil Kumar, S., et al., A visible light-cross-linkable, fibrin–gelatin-based bioprinted construct with human cardiomyocytes and fibroblasts. ACS biomaterials science & engineering, 2019. 5(9): p. 4551-4563.

 doi:10.20944/preprints202306.0887.v1



24. Sharma, R., et al., Physical and Mechanical Characterization of Fibrin-Based Bioprinted Constructs Containing Drug-Releasing Microspheres for Neural Tissue Engineering Applications. Processes, 2021. 9(7): p. 1205.
25. Bilkic, I., et al., Development of an extrusion-based 3D-printing strategy for clustering of human neural progenitor cells. Heliyon, 2022. 8(12): p. e12250.
26. Winbo, A., J.L. Ashton, and J.M. Montgomery, Neuroscience in the heart: Recent advances in neurocardiac communication and its role in cardiac arrhythmias. The International Journal of Biochemistry & Cell Biology, 2020. 122: p. 105737.